HOKKAIDO UNIVERSITY

| | |
|---|---|
| Title | Conformational change in full-length mouse prion: a site-directed spin-labeling study. |
| Author(s) | Inanami, Osamu; Hashida, Shukichi; Iizuka, Daisuke; Horiuchi, Motohiro; Hiraoka, Wakako; Shimoyama, Yuhei; Nakamura, Hideo; Inagaki, Fuyuhiko; Kuwabara, Mikinori |
| Citation | Biochemical and Biophysical Research Communications, 335(3), 785-792<br>https://doi.org/10.1016/j.bbrc.2005.07.148 |
| Issue Date | 2005-09-30 |
| Doc URL | http://hdl.handle.net/2115/27969 |
| Type | article (author version) |
| File Information | BBRC335-3.pdf |

Instructions for use

Hokkaido University Collection of Scholarly and Academic Papers : HUSCAP

# Conformational change in full-length mouse prion: A site-directed spin-labeling study

[a,f,g,*]Osamu Inanami, [a,f]Shukichi Hashida, [a]Daisuke Iizuka, [a,f]Motohiro Horiuchi, [b]Wakako Hiraoka, [c,g]Yuhei Shimoyama, [d,g]Hideo Nakamura, [e]Fuyuhiko Inagaki and [a]Mikinori Kuwabara

[a]Laboratory of Radiation Biology, Department of Environmental Veterinary Medical Sciences, Graduate School of Veterinary Medicine, Hokkaido University, Sapporo 060-0818, Japan

[b]Department of Physics, School of Science and Technology, Meiji University, Kawasaki 214-8571, Japan

[c]Soft-Matter Physics Laboratory, Department of Materials Science and Engineering, Muroran Institute of Technology, Muroran 050-8585, Japan.

[d]Laboratory of Chemistry, Faculty of Education, Hokkaido University of Education, Hakodate 040-8567, Japan

[e]Department of Structural Biology, Graduate School of Pharmaceutical Sciences, Hokkaido University, Sapporo 060-0812, Japan

[f]COE program, Program for Excellence of Zoonosis Control, Sapporo 060-0818, Japan

[g]CREST-JST, Multi-Quantum Coherence ESR Project, Muroran 050-8585 and Hakodate 040-8567, Japan

*Corresponding Author:

Phone: +81-11-706-5236

Fax: +81-11-706-7373

E-mail: inanami@vetmed.hokudai.ac.jp

Laboratory of Radiation Biology, Department of Environmental Veterinary Medicine, Graduate School of Veterinary Medicine, Hokkaido University, Kita 18-Jo Nishi 9-Chome, Sapporo 060-0818, Japan

**Abstract**

The structure of the mouse prion (moPrP) was studied using site-directed spin-labeling electron spin resonance (SDSL-ESR). Since a previous NMR study by Hornemanna *et al.*, [FEBS Lett. 413 (1997) 277-281] has indicated that N96, D143 and T189 in moPrP are localized in a $Cu^{2+}$ binding region, Helix1 and Helix2, respectively, three recombinant moPrP mutations (N96C, D143C and T189C) were expressed in an *E. coli.* system, and then refolded by dialysis under low pH and purified by reverse-phase HPLC. By using the preparation, we succeeded in preserving a target cystein residue without alteration of the α-helix structure of moPrP and were able to apply SDSL-ESR with a methane thiosulfonate spin label (MTSSL) to the full-length prion protein. The rotational correlation times (τ) of 1.1, 3.3 and 4.8 nsec were evaluated from the X-band ESR spectra at pH 7.4 and 20°C for N96R1, D143R1 and T189R1, respectively. τ reflects the fact that the $Cu^{2+}$ binding region is more flexible than Helix1 or Helix2. ESR spectra recorded at various temperatures revealed two phases together with a transition point at around 20°C in D143R1 and T189R1, but not in N96R1. With the variation of pH from 4.0 to 7.8, ESR spectra of T189R1 at 20°C showed a gradual increase of τ from 2.9 to 4.8 nsec. On the other hand, the pH-dependent conformational changes in N96R1 and D143R1 were negligible. These results indicated that T189 located in Helix2 possessed a structure sensitive to physiological pH changes; simultaneously, N96 in the $Cu^{2+}$ binding region and D143 in Helix1 were conserved.

**Keywords:** site-directed spin-labeling; electron spin resonance; prion; conformational change; pH-sensitive region.

**Introduction**

The cellular prion protein ($PrP^{C}$) is a glycosylphosphatidylinositol (GPI)-plasma membrane-anchored protein whose function is still under debate [1-10]. Conversion of $PrP^{c}$ from an α-helix- to a β-sheet-rich structure (the scrapie prion protein, $PrP^{Sc}$) causes relevant biophysical changes to the protein that have been related to brain dysfunction in prion diseases [1-3]. The mechanisms involved in the conversion are unknown. However, accumulating evidence suggests that the process occurs after $PrP^{c}$ reaches the plasma membrane, and it may involve entry of $PrP^{c}$ into intracellular acidic organelles [4-10].

As shown in Fig. 1A, the prion protein of the mouse, moPrP, consists of 208 amino acids (residues 23–231). It contains a carboxy-terminal domain, moPrP(121–231), which represents an autonomous folding unit with three α-helices (Helix1, Helix2 and Helix3) and a two-stranded antiparallel β-sheet [1-3, 11-13]. In the full-length prion protein, moPrP(23–231), comparison of near-UV circular dichroism (CD), fluorescence and one-dimensional $^{1}$H-NMR spectra of moPrP(23–231) and moPrP(121–231) shows that amino-terminal segment 23–120, which includes the five characteristic octapeptide repeats, does not contribute measurably to the manifestation of the three-dimensional structure as detected [7]. Development of techniques for analysis of the structural and conformational changes in the amino-terminal region of moPrP is of great importance, because the amino-terminal region acts as a $Cu^{2+}$ binding domain [11] and $Cu^{2+}$ ions modulate various biological functions of prions such as the cellular enzymatic activity of superoxide dismutase (SOD) [14], signal transduction [15], shedding of $PrP^{c}$ [16] and conversion to $PrP^{sc}$ [17]. Recently, site-directed spin labeling (SDSL) together with electron spin resonance (ESR) spectroscopy has proven to be a practical method for determining the secondary structure and molecular orientation; surfaces of tertiary interactions; inter-residue distances and the chain topologies of various proteins [18-21]. SDSL involves the introduction of a spin-labeled side chain into protein sequences, usually through cysteine substitution mutagenesis, followed by reaction with a sulfhydryl-specific nitroxide reagent such as a methane thiosulfonate spin label (MTSSL) (Fig. 1B). Although SDSL-ESR is widely recognized as a useful method for structural analysis and domain dynamics of a number of membrane and soluble proteins,

there are no reports about the application of this technique to detection of conformational changes in $PrP^c$.

In the present study, to obtain the information about pH- and temperature-dependent conformational changes of typical domains in PrP, we employed the SDSL-ESR technique. We targeted the amino acid residues of N96, D143 and T189 of recombinant moPrP for the SDSL study, since previous NMR studies showed that N96, D143 and T189 in moPrP were localized in a $Cu^{2+}$ binding region around H95, Helix1 and Helix2, respectively [7, 12, 13].

## Materials and Methods

*Materials*. (1-Oxy-2,2,5,5-tetramethyl-3-pyrroline-3-methyl)Metanethiosulfonate (MTSSL) was purchased from Toronto Research Chemicals (ON, Canada). *E. coli* BL21(DE3)*LysS* and isopropylthio-β-$_D$-galactoside (IPTG) were from Invitrogen (CA, USA). The TSKgel Phenyl-5PW RP column was from TOSOH (Tokyo, Japan). Other reagents were from Wako Pure Chemical, Co. (Tokyo, Japan)

*Construction of moPrP mutants*. cDNA encoding moPrP codons 23–231 was cloned into BamHI/EcoRI sites of pRSETb as described previously [22]. To generate the mutant moPrP containing a single amino acid substitution at codon 96 (Asn to Cys) , 143 (Asp to Cys) or 189 (Thr to Cys), we used the PCR-based site-directed mutagenesis method described by Imai *et al.* [23]. The change of the codon by cystein substitution mutagenesis was confirmed using a DNA sequencer (CEQ8800, Beckman).

*Expression and purification of recombinant moPrP mutants*. The expression plasmids were introduced into *E. coli* BL21(DE3)*LysS*. Protein expression was induced by adding IPTG to a final concentration at 0.5 mM. Four to six hours after induction, bacterial cells were collected and inclusion bodies were prepared as described elsewhere [24]. The inclusion bodies from BL21(DE3)*LysS* transformed with expression plasmids were solubilized with 6 M GdnHCl in 20 mM phosphate buffer (pH 7.8). The recombinant

moPrP was further purified by $Ni^{2+}$-immobilized metal affinity chromatography using $Ni^{2+}$-charged chelating sepharose (Qiagen) and a stepwise elution gradient from pH 6.5 to pH 4.3 in the presence of 8 M urea. After dialysis against 10 mM acetate buffer (pH 4.0) for 48 h, recombinant moPrP containing an intramolecular disulfide bond was purified by reverse-phase HPLC using TSKgel Phenyl-5PW RP and a 30-50% linear gradient of acetonitrile with 0.05% trifluoroacetic acid. The purified recombinant moPrP was dialyzed against 10 mM acetate buffer (pH 4.0) and stored at -20°C until use. The protein concentration was determined by UV absorption at 276 nm using an extinction coefficient of 39,425 $cm^2$ $M^{-1}$. Protein purity was analyzed by sodium dodecyl sulfate polyacrylamide gel electrophoresis (SDS-PAGE) followed by Commasie Brilliant Blue staining. All mutants were at least 95% pure as judged by the SDS-PAGE.

*Circular dichroism (CD).* Far-UV CD spectra were recorded on a JASCO J-820 spectropolarimeter with a protein concentration of 0.3 mg/ml in 1 mm pathlength cuvettes using a scan speed of 50 nm/min and a response time of 2 sec. Multiple scans were averaged (typically n=6).

*Spin-labeling of moPrP mutants***.** To label the moPrP mutants with MTSSL, a 10-fold molar excess of MTSSL was added to each moPrP mutation in 10 mM acetate buffer (pH 4.5) and the sample was incubated in the dark for 12 h - 24 h at 4°C for solvent-accessible sites. The free spin label was removed from the protein using a microdializer (Nippon Genetics) and spin-labeled moPrP was concentrated by centrifugal concentrator (Vivascience). To confirm the site-specific spin-labeling for the cystein residue created by mutagenesis, the sample solution containing the spin-labeled moPrP mutant was digested for 3 h - 24 h at 37°C with 1 µg/ml trypsin (Promega) in 50 mM Tris-HCl, pH 8.0, 1 mM $CaCl_2$, and the fragment mass was examined with a matrix-assisted laser desorption ionization (MALDI) mass spectrometer (AutoFLEX, Bruker) equipped with a 337 nm laser source. In all mutants, there was an increase of about m/z=184 by addition of a side chain (R1) of the labeling compound as expected if specifically incorporated MTSSL was detected in each fragment containing the substituted cystein (data not shown).

*ESR spectroscopy*. The pH change of the sample solution was carried out by dialysis of the sample against 10 mM acetate buffer from pH 4.0 to pH 6.0 or 10 mM Tris-HCl buffer from pH 6.5 to pH 8.0. For ESR spectroscopy, 70 µl of spin-labeled moPrP solution was put into a quartz flat cell (RST-DVT05; 50 mm x 4.7 mm x 0.3 mm, Radical Research Inc.). Spectra were detected using a JEOL-RE X-band spectrometer (JEOL) connected with a cylindrical TE011 mode cavity (JEOL). All the ESR spectra were recorded at the temperature range of 5°C - 60°C maintained by a temperature controller (ES-DVT4, JEOL). We used a field modulation of 0.2 mT operating at 100 kHz, an incident microwave power of 5 mW and a field sweep of 10 mT. Three field sweeps were averaged for each acquired spectrum by using the Win-Rad Radical Analyzer System (Radical Research Inc.). The rotational correlation time ($\tau$) was reported by using following equation described by Kivelson [25]).

$$\tau_{(nsec)} = a_o \, \delta H_{(0)} \left( \sqrt{h_{(0)}/h_{(+1)}} - 1 \right) \qquad (1)$$

Here $\delta H_{(0)}$ is the width of the central peak of the nitroxide signal (in mT); $h_{(0)}$ and $h_{(+1)}$ are lineheights of the spectral peaks for the quantum numbers of M=0 and +1, and we employed a value of 6.5 for the constant $a_0$. The practical evaluation of $\tau$ was performed by the spin-label calculator system of the Win-Rad Radical Analyzer System (Radical Research Inc.).

## Results

### Spin-labeling of recombinant moPrP

For the SDSL-ESR experiment, refolding of recombinant moPrP mutants isolated from inclusion bodies of *E. coli.* was achieved by dialysis against 10 mM acetate buffer (pH 4.0) and the native form of moPrP was isolated by reverse-phase HPLC. The native form of recombinant moPrP is generally defined by the oxidative formation of its single disulfide bond (Cys178-Cys213) and characterized by a typical

α-helical far-UV CD spectrum, with minima at 208 nm and 222 nm [7, 26]. These two minima at 208 nm and 220 nm are reported to disappear if the disulfide bond between Cys179 and Cys214 is destroyed by mutagenesis or treatment with a reducing reagent such as DTT [26]. Therefore, we first recorded far-UV CD spectra of recombinant moPrP mutants in order to confirm that the α-helix content of recombinant moPrP mutants was similar to that of recombinant wild-type moPrP. Figure 2 shows far-UV CD spectra obtained from wild-type, N96C, D143C and T189C moPrP. Two minima, at about 208 and 220 nm, typical of a mainly a helix structure protein, were clearly observed in all samples and there were no differences in the spectra between wild-type moPrP and moPrP mutants (N96C, D143C and T189C). Moreover, SDS-PAGE with or without dithiothreitol (DTT) showed that no intermolecular disulfide linkage was produced in any moPrP mutant (data not shown). Therefore, our results indicated that the mutagenesis did not affect the α-helical structure of recombinant PrP by preferential formation of a disulfide bond between Cys179 and Cys214 and that the cystein residue created by mutagenesis was preserved during the oxidative refolding.

**Temperature-dependent conformational changes of moPrP**

The ESR spectra detected from MTSSL bonded with moPrP(wild-type), moPrP(N96C), moPrP(D143C) and moPrP(T189C) were shown in Fig. 3. These ESR spectra are recorded at pH 7.4 at 20$^{o}$C. In PrP$^{c}$(wild-type), no signals derived from the nitroxide radical of MTSSL were not detected, indicating there were no free cystein residues, whereas a triplet ESR signal due to the nitroxide moiety undergoing various dynamic changes was clearly seen in moPrP(N96C), moPrP(D143C) and moPrP(T189C). The rotational correlation times (τ) of 1.1, 3.3 and 4.8 nsec were evaluated from these ESR spectra of moPrP(N96C), moPrP(D143C) and moPrP(T189C), respectively. This indicated that the $Cu^{2+}$ binding region was more flexible than the Helix1 region containing D139 or Helix2 containing T189. Furthermore, the line shapes of ESR spectra shown in Fig. 4A-C showed the temperature-dependent variation. There were some peaks in the outermost of the ESR spectrum of T189R1 at 10$^{o}$C and 20$^{o}$C, which were due to the parallel component ($A_{//}$) of the hyperfine tensor. These peaks, as shown by arrows in Fig. 4C, therefore indicated

immobilization of the nitroxide moiety in the local region of T189R1. In fact, these peaks vanished at higher temperatures (*e.g.* 30°C). The rotational correlation times (τ) were calculated and plotted as a function of temperature at pH 4.4, pH 6.4 and pH 7.4 in Fig. 4D-F. In all moPrP mutants, an increase of temperature induced a decrease in τ, which indicated rapid tumbling of the nitroxide moiety. Two phases, a steeper decline of τ at from 5°C to 20°C and a gentle decline at temperatures >20°C, were observed in moPrP(D143C) and moPrP(T189C) at pH 4.4, pH 6.4 and pH 7.4. We found the presence of a breaking point or a phase transition at around 20°C. The results of slower correlation times found at 10 and 20°C explain the appearance of $A_{//}$-peaks in the outermost field in moPrP(T189C). However, the phase transition point at 20°C was not well-defined in moPrP(N96C) at any pH.

**pH-Dependent conformational changes in moPrP**

As shown in Fig. 4F, we found a difference in τ between pH 7.4 and pH 4.4 in moPrP(T189R1), although there were no pH-dependent differences in τ of moPrP(N96C) and moPrP(D143C) as shown in Fig. 4D and 4E. Figure 5 shows typical ESR spectra in pH 4.4 solution and pH 7.4 solution of moPrP(T189R1) recorded at 20°C. The immobilization of the nitroxide moiety at pH 7.4 is obvious in comparison with that at pH 4.4. Furthermore, to define the pH-dependency, we examined the lineshape variation in the ESR spectra of moPrP(T189R1) and moPrP(T189R1) solutions whose pHs were gradually changed from pH 4.0 to pH 7.8 by dialysis. As shown in Fig. 5B, two regions were observable in moPrP(T189R1), a steep increase phase at pH 4.0 - pH 4.8 and a gradual increase phase at pH 5.4 - pH 7.8. Stone *et al*. have also shown similar pH-dependent phase transition at around pH 4.0 in spin-labeled BSA [27]. At temperatures from 5°C to 20°C, we found a breaking point between the two phases at around pH 5.0 that was clearer than those seen at temperatures >30°C. These results indicated that the region around T189R1 was more pH-sensitive than the N96R1 and D189R1 regions.

**Discussion**

**Preparation procedures of SDSL.**

Site-directed spin labeling is one of the most powerful methods for investigating structure and conformational switching in soluble and membrane proteins [18, 20]. Analysis of nitroxide side chain dynamics in spin-labeled proteins reveals contributions from fluctuations in the backbone, dihedral angles and rigid-body motions of α-helices [18-21]. With this technique, however it is necessary that free cystein residues be substituted for alanine or serine residues for specificity in the reaction of MTSSL with the target cystein residue created by mutagenesis. The native mouse, hamster, bovine and human prion proteins do not have free cystein residues, but a disulfide linkage is known to exist between Helix2 and Helix3 and to be essential for formation of the three helix structures, which are important in refolding prion secondary structures [26].

Although Lundberg *et al.* have reported the time-dependent changes of the ESR spectrum of a short synthetic prion-derived penta-peptide, AGAACAGA with Cys117 substituted for Ala117 in PrP(113-120) [28], there have been few reports on structural analysis by SDSL for the full-length proteins such as PrP having an intracellular disulfide linkage. Application of the SDSL technique is impossible for full-length native PrP protein, because cystein residues newly created by mutagenesis interfere with the formation of the disulfide linkage between Helix2 and Helix3. For this reason, the present experiment employed dialysis against low pH buffer, and reverse-phase HPLC for the refolding and the purification procedures. We demonstrated that the recombinant moPrP produced by this preparation could be successfully used for SDSL experiments as proved by the following evidence. First, far-UV-CD spectroscopy, as shown in Fig. 2, clearly demonstrated that the content of the helical structures in moPrP mutants was similar to that in native moPrP. This fact indicates the preferential formation of a disulfide linkage between Cys178 and Cys213, because the abrogation of this disulfide linkage never gives two minima at 208 nm and 220 nm in far-UV-CD spectra [26]. Second, the possibility of dimer formation due to intermolecular disulfide-linkage between cystein residues newly created by mutagenesis was ruled out because SDS-PAGE of recombinant moPrP without the reducing reagent showed a single band

(data not shown). Third, MALDI-TOF mass spectroscopic data showed increases of ca. m/z = 184 due to a side chain of the nitroxide moiety in the fragment after the tryptic digestion of spin-labeled moPrP mutants (data not shown). Thus, we were able to preserve the target cystein created by mutagenesis, and succeeded for the first time in applying SDSL to the full length prion protein.

**Conformational changes of $Cu^{2+}$ binding region and α-helix regions.**

Prion protein was reported to contain an amino terminal $Cu^{2+}$ binding octarepeat segment and a carboxy-terminal domain, three α-helices (Helix1, Helix2 and Helix3) and a two-stranded antiparallel β-sheet [1-3, 11-13]. The amino acid residues of N96, D143 and T189 in moPrP have been chosen as targets for SDSL. Recently, in addition to the octapeptide repeat region, a novel $Cu^{2+}$ binding structure between H95 and H110 was reported [29] and N96 is close to this region. D143 is located in the initial part of Helix1 and D189 in the end part of Helix2. A marked difference in rotational correlation times was observed by the spin-labeled positions (Fig. 3). NMR data of hamster PrP(90-231) showed that the region from 90-124, which includes the characteristic octapeptide repeat sequence, was clearly flexible with large negative NOEs and local correlation times of less than 1 nsec. This is due to the fact that residues do not form part of any stable secondary or tertiary fold and are highly flexible [30]. Our ESR spectrum of moPrP(N96R1) also showed that the $Cu^{2+}$ region around H95 reflected more flexible motion as compared with the rigid-body motion of helix structure revealed by ESR-line-shapes from moPrP(D143R1) and moPrP(T189R1).

Our data showed that the end part of Helix2 around T189R1 was highly pH-sensitive compared to the $Cu^{2+}$ binding region around N96R1 and the first part of Helix1 around T189R1 (Fig. 4D-F and Fig. 5). The conversion from $PrP^{c}$ to $PrP^{Sc}$ is a post-transcriptional process that appears via the endosome pathway [4, 5, 9] and/or caveolae-like domains [10], both of which are acidic. Lower pH also accelerates conversion from $PrP^{c}$ to $PrP^{Sc}$ in a cell-free system [30]. Recently, Swietnicki *et al*. have shown that incubation of the recombinant prion protein under mildly acidic conditions (pH 5 or below) in the presence of low concentrations of guanidine hydrochloride produces a transition to $PrP^{Sc}$-like beta-sheet-rich oligomers that show fibrillar

morphology and increased resistance to proteinase K digestion [32]. Since low pH plays a role in facilitating the conformational change that ultimately results in $PrP^{Sc}$ formation, some parts of Helix2 may be candidates for the pH-sensitive region associated with $PrP^{Sc}$ conversion. In this region, we found a phase transition point at around pH 5.0 as shown in Fig. 5B. This evoked the induction of rapid structural change in the end part of Helix2 below pH 5.0. For analysis of the precise mechanism of pH-induced conformational changes in this region, further studies using the SDSL-ESR technique using variety of recombinant moPrP mutants created on Helix2 will be necessary.

**ESR of spin label dynamics.**

The mobility of the spin label moiety attached to a protein can be quantified in terms of the rotational correlation times in the case of weakly immobilized labels ($\tau = 10^{-9} – 10^{-10}$ sec). $\tau$ is determined by the relative linewidths based upon relaxation theory and is given by Eq. 1 (*vide infra*). In the equation, the lineheights are used instead of the linewidths, because the former are easy to measure accurately. The constant factor $a_o$ in Eq. 1 is derived from the g-factor and hyperfine anisotropies. For these reasons, Eq. 1 is only applicable to a spin label signal that possesses three well-defined lines with longitudinal (or up and down) symmetry and no anisotropic outermost lines due to the $g_{//}$ anisotropy. In the present study, we applied Eq. 1 to the rapid tumbling of the weakly immobilized regime of the spin label dynamics.

**Acknowledgements**

This work was supported in part by Grants-in-Aid for Basic Scientific Research from the Ministry of Education, Culture, Sports, Science and Technology of Japan (No. 17380178 [O.I.], No. 17580275 and No. 17658126 [M.K.]). O.I., Y.S. and H.N thank the Research Grants from COE program and CREST-JST program.

**References**

[1] S. B. Prusiner, Prions, Proc. Natl. Acad. Sci. USA 95 (1998) 13363-13383.

[2] C. Weissmann, Molecular genetics of transmissible spongiform encephalopathies, J. Biol. Chem. 274 (1999) 3-6.

[3] A. Aguzzi, M. Glatzel, F. Montrasio, M. Prinz and F.L. Heppner, Interventional strategies against prion diseases. Nat. Rev. Neurosci. 2 (2001) 745-749.

[4] B. Caughey and G.J. Raymond, The scrapie-associated form of PrP is made from a cell surface precursor that is both protease- and phospholipase-sensitive, J. Biol. Chem. 266 (1991) 18217-18223.

[5] B. Caughey, G.J. Raymond, D. Ernst, and R.E.Race, N-terminal truncation of the scrapie-associated form of PrP by lysosomal protease(s): implications regarding the site of conversion of PrP to the protease-resistant state, J. Virol. 65 (1991) 6597-6603.

[6] A. Taraboulos, M. Scott, A. Semenov, D. Avrahami, L. Laszlo, S. B. Prusiner, and D. Avrahami, Cholesterol depletion and modification of COOH-terminal targeting sequence of the prion protein inhibit formation of the scrapie isoform, J. Cell Biol. 129 (1995) 121-132.

[7] S. Hornemanna, C. Korthb, B. Oeschb, R. Rieka, G. Widera, K. Wüthricha and R. Glockshubera, Recombinant full-length murine prion protein, mPrP(23–231): purification and spectroscopic characterization, FEBS Lett. 413 (1997) 277-281.

[8] A.C.Magalhaes, J,A, Silva, K.S. Lee, V.R. Martins, V.F. Prado, S.S. Ferguson, M.V. Gomez, R.R. Brentani and M.A. Prado, Endocytic intermediates involved with the intracellular trafficking of a fluorescent cellular prion protein. J. Biol. Chem. 277 (2002) 33311-33318.

[9] D.R. Borchelt, A. Taraboulos and S.B. Prusiner, Evidence for synthesis of scrapie prion proteins in the endocytic pathway, J. Biol. Chem. 267 (1992 ) 16188-16199.

[10] M. Vey, S. Pilkuhn, H. Wille, R. Nixon, S.J. DeArmond, E.J. Smart, R.G. Anderson, A. Taraboulos and S.B. Prusiner, Subcellular colocalization of the cellular and scrapie prion proteins in caveolae-like membranous domains, Proc. Natl. Acad. Sci. USA 93 (1996) 14945-14949.

[11] C.S. Burns, E. Aronoff-Spencer, G. Legname, S.B. Prusiner, W.E. Antholine, G.J. Gerfen, J. Peisach and G.L. Millhauser. Copper coordination in the full-length, recombinant prion protein, Biochemistry 42 (2003) 6794-6803.

[12] M. Billeter, R. Riek, G. Wider, S. Hornemann, R. Glockshuber and K. Wuthrich, Prion protein NMR structure and species barrier for prion diseases, Proc. Natl. Acad. Sci. USA 94 (1997):7281-7285.

[13] R. Riek, S. Hornemann, G. Wider, M. Billeter, R. Glockshuber and K. Wuthrich. NMR structure of the mouse prion protein domain PrP(121-321), Nature 382(1996) 180-182.

[14] W. Rachidi, D. Vilette, P. Guiraud, M. Arlotto, J. Riondel, H. Laude, S. Lehmann and A. Favier, Expression of prion protein increases cellular copper binding and antioxidant enzyme activities but not copper delivery, J. Biol. Chem. 278 (2003) 9064-9072.

[15] C. Spielhaupter and H.M. Schatzl, $PrP^C$ directly interacts with proteins involved in signaling pathways, J. Biol. Chem. 276 (2001) 44604-44612.

[16] E.T. Parkin, N.T. Watt, A.J. Turner and N.M. Hooper, Dual mechanisms for shedding of the cellular prion protein, J. Biol. Chem. 279 (2004) 11170-1178.

[17] N. Hijazi, Y. Shaked, H. Rosenmann, T. Ben-Hur and R. Gabizon, Copper binding to $PrP^C$ may inhibit prion disease propagation, Brain Res. 993 (2003) 192-200.

[18] W.L. Hubbell, C. Altenbach, C.M. Hubbell and H.G. Khorana, Rhodopsin structure, dynamics, and activation: a perspective from crystallography, site-directed spin labeling, sulfhydryl reactivity, and disulfide cross-linking, Adv. Protein Chem. 63 (2003) 243-290.

[19] R. Biswas, H. Kuhne, G.W. Brudvig and V. Gopalan, Use of EPR spectroscopy to study macromolecular structure and function, Sci. Prog. 84 (2001) 45-67.

[20] W.L. Hubbell, D.S. Cafiso and C. Altenbach, Identifying conformational changes with site-directed spin labeling, Nat. Struct. Biol. 7 (2000) 735-739.

[21] H.S. Mchaourab, M.A. Lietzow, K. Hideg and W.L. Hubbell, Motion of spin-labeled side chains in T4 lysozyme. Correlation with protein structure and dynamics, Biochemistry 35 (1996) 7692-76704.

[22] C.L. Kim, A. Umetani, T. Matsui, N. Ishiguro, M. Shinagawa and M. Horiuchi, Antigenic characterization of an abnormal isoform of prion protein using a new diverse panel of monoclonal antibodies, Virology 320 (2004 1) 40-51.

[23] Y. Imai, Y. Mastushima, T. Sugimura and M. Terada, A simple and rapid method for generating a deletion by PCR, Nucleic Acid Res. 19 (1991) 2785.

[24] J. Sambrook, E.F. Fritsch and T. Maniatis, Molecular Cloning: A Laboratory Manual, (1989) Cold Spring Harbor Press, Cold Spring Harbor, NY.

[25] D. Kivelson, Theory of ESR linewidths of free radicals, J. Chem. Phys. 33 (1960) 1094-1106.

[26] N.R. Maiti and W.K. Surewicz, The role of disulfide bridge in the folding and stability of the recombinant human prion protein, J. Biol. Chem. 276 (2001) 2427-2431.

[27] T. J. Stone. T. Buckman, P. L. Nordio and H. M. McConnel, Spin-labeled biomolecules, Proc. Natl. Acad. Sci. USA 54 (1965) 1010-1017

[28] K.M. Lundberg, C.J. Stenland, F.E. Cohen, S.B. Prusiner and G.L. Millhauser, Kinetics and mechanism of amyloid formation by the prion protein H1 peptide as determined by time-dependent ESR, Chem. Biol. 4 (1997) 345-355.

[29] C.E. Jones, S.R. Abdelraheim, D.R. Brown and J.H. Viles, Preferential $Cu^{2+}$ coordination by His96 and His111 induces beta-sheet formation in the unstructured amyloidogenic region of the prion protein, J. Biol. Chem. 279 (2004) 32018-32027.

[30] H. Liu, S. Farr-Jones, N.B. Ulyanov, M. Llinas, S. Marqusee, D. Groth, F.E. Cohen, S.B. Prusiner and T.L. James, Solution structure of Syrian hamster prion protein rPrP(90-231), Biochemistry 38 (1999) 5362-5377.

[31] D.A. Kocisko, S.A. Priola, G.J. Raymond, B. Chesebro, P.T.Jr. Lansbury and B. Caughey, Species specificity in the cell-free conversion of prion protein to protease-resistant forms: a model for the scrapie species barrier, Proc. Natl. Acad. Sci. USA 92 (1995) 3923-3927.

[32] W. Swietnicki, M. Morillas, S.G. Chen, P. Gambetti and W.K. Surewicz. Aggregation and fibrillization of the recombinant human prion protein huPrP90-231, Biochemistry 39 (2000) 424-431.

**Legends to Figures**

**Figure 1** (A) Three-dimensional rendering of PrP (61-231) [11] and the target sites (N96, D143 and T189) for site-directed spin-labeling (SDSL). (B) The reaction scheme of the metanethiosulfonate spin labeling reagent with cystein residue to yield the R1 side chain attached to the PrP.

**Figure 2** Circular dichroism (CD) spectra obtained from 0.3 mg/ml of moPrP (wild-type), moPrP (N96C), moPrP (D143C) and moPrP (T189C).

**Figure 3** X-band ESR spectra of spin-labeled recombinant moPrP mutants. After reaction of MTSSL with moPrP (wild-type) (A), moPrP (N96C) (B), moPrP(D143C) (C) and moPrP (T189C) (D), the free spin labeling compound was removed by dialysis against 10 mM acetate buffer (pH 4.0) for 48 h. pH of the sample was adjusted to 7.4 by dialysis against 10 mM Tris-HCl buffer for 4 hours. ESR spectra were recorded by an X-band ESR spectrometer with a field modulation of 0.2 mT, operating at 100 kHz, an incident microwave power of 5 mW and a field sweep of 10 mT.

**Figure 4** X-band ESR spectra of recombinant moPrP (N96R1) (A), moPrP (D143R1) (B) and moPrP (T189R1) (C) at 10°C, 20°C, 30°C, 40°C and 50°C. The rotational correlation times, $\tau$ (nsec) were evaluated from ESR spectra of moPrP (N96R1) (D), moPrP (D143R1) (E) and moPrP (T189R1) (F) at various temperatures at pH4.4, 6.4 and 7.4.

**Figure 5** (A) X-Band ESR spectra of moPrP (T189R1) at 20°C and pH 4.4 (black line) and pH 7.4 (red line). (B) The rotational correlation time, $\tau$ (nsec) at various pHs as detected by the ESR spectra of moPrP (T189R1) at from 5°C to 60°C.

Figure
Click here to download high resolution image

Fig. 1

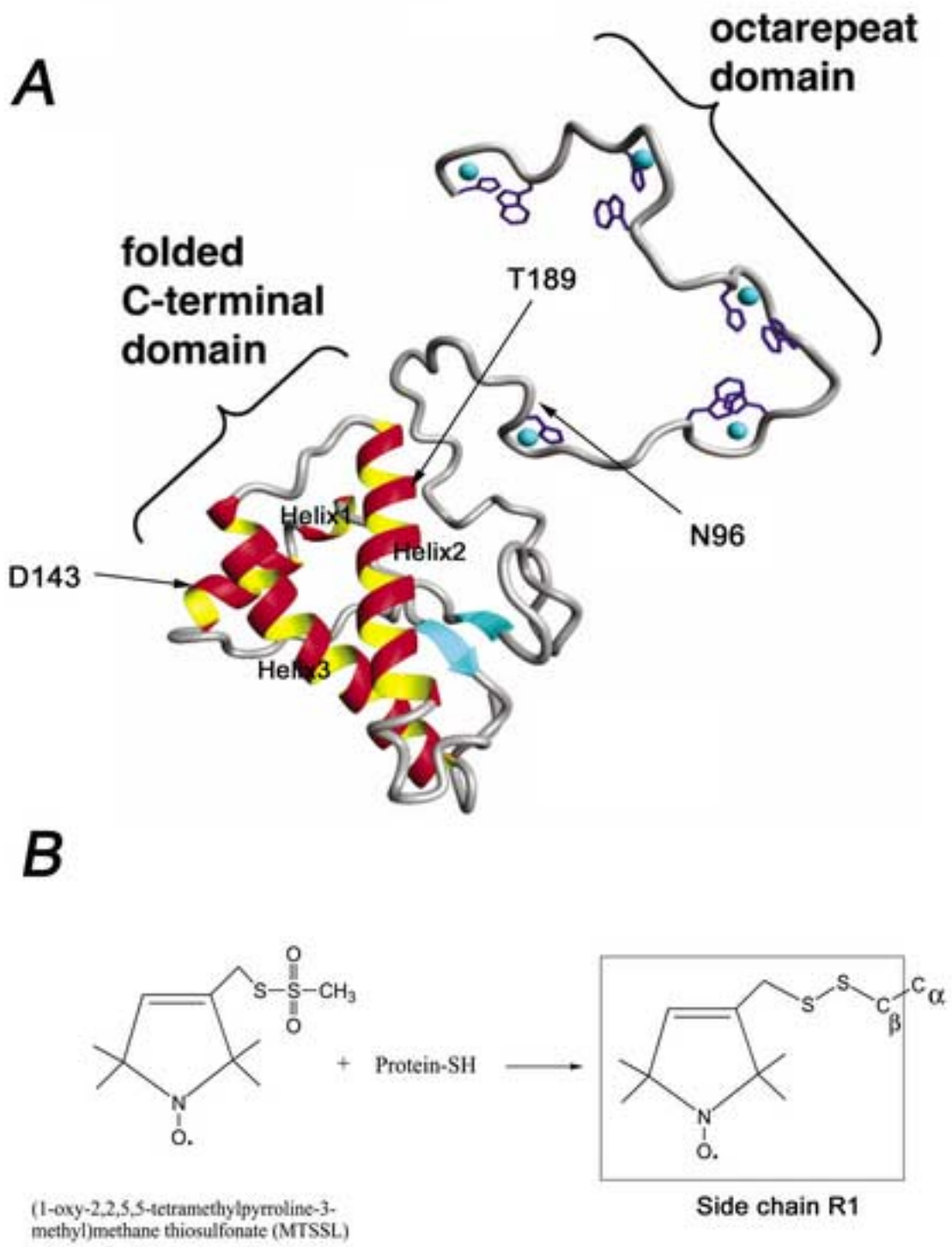

Figure
Click here to download high resolution image

Fig.2

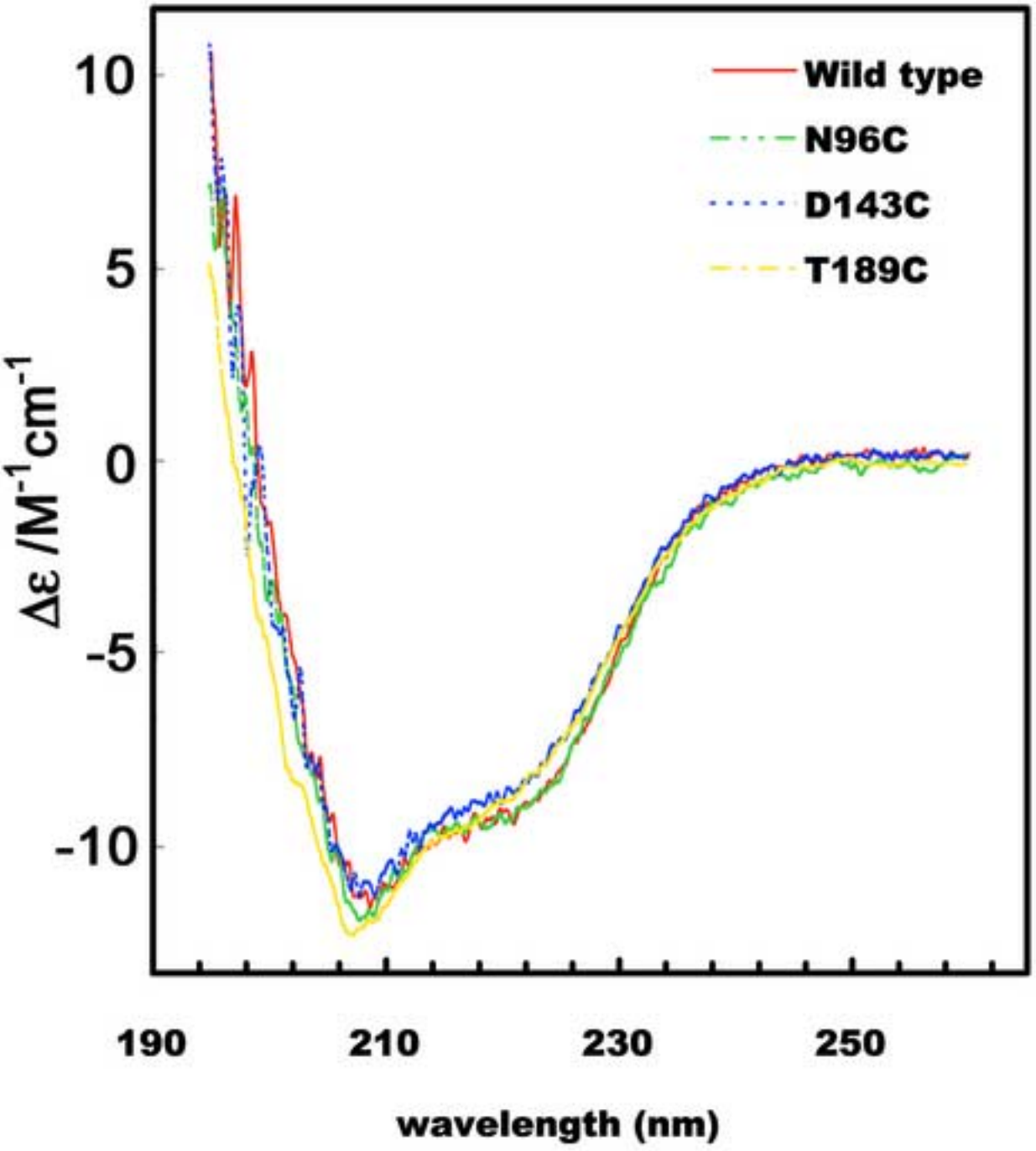

Figure
Click here to download high resolution image

Fig.3

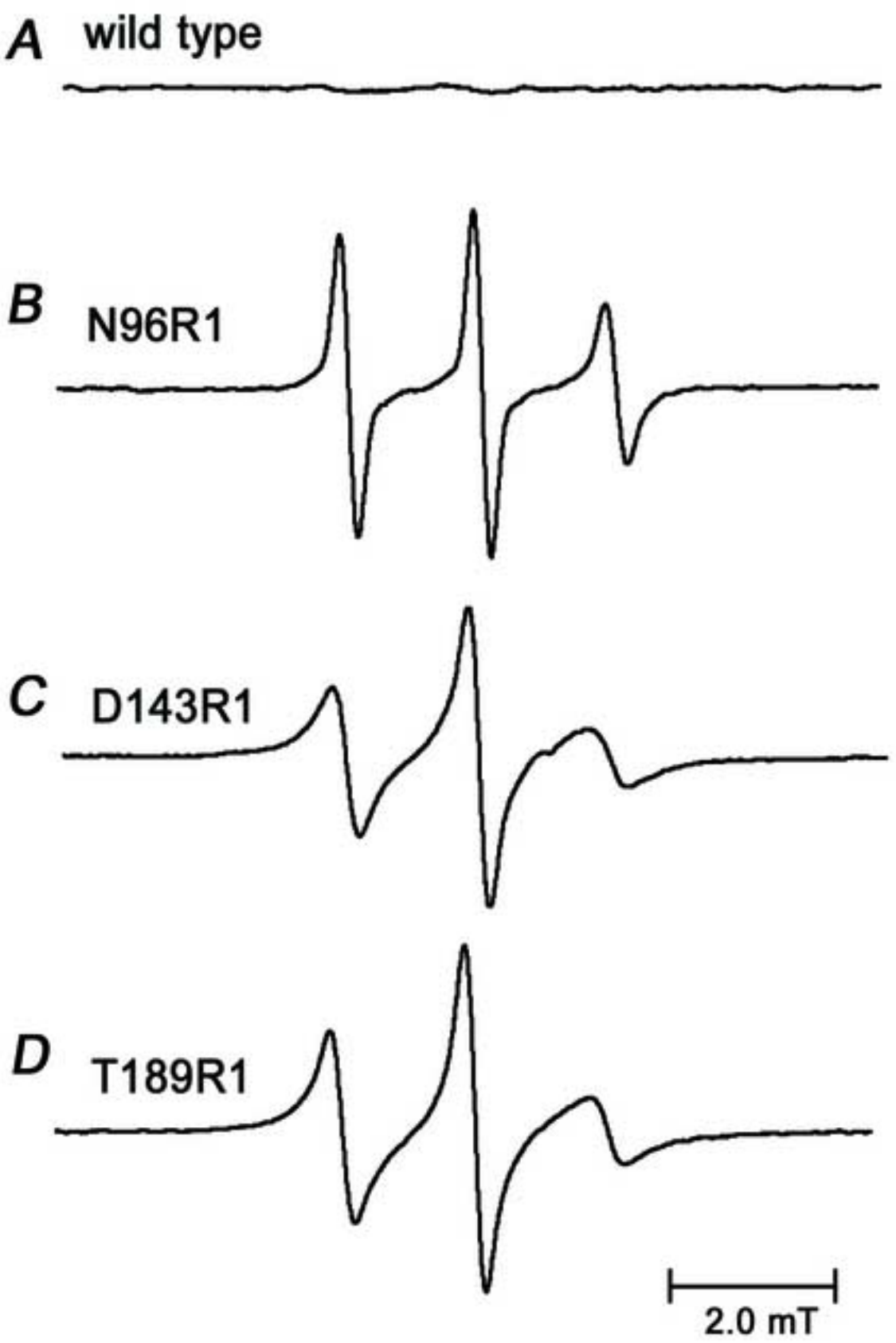

Figure
Click here to download high resolution image

Fig.4

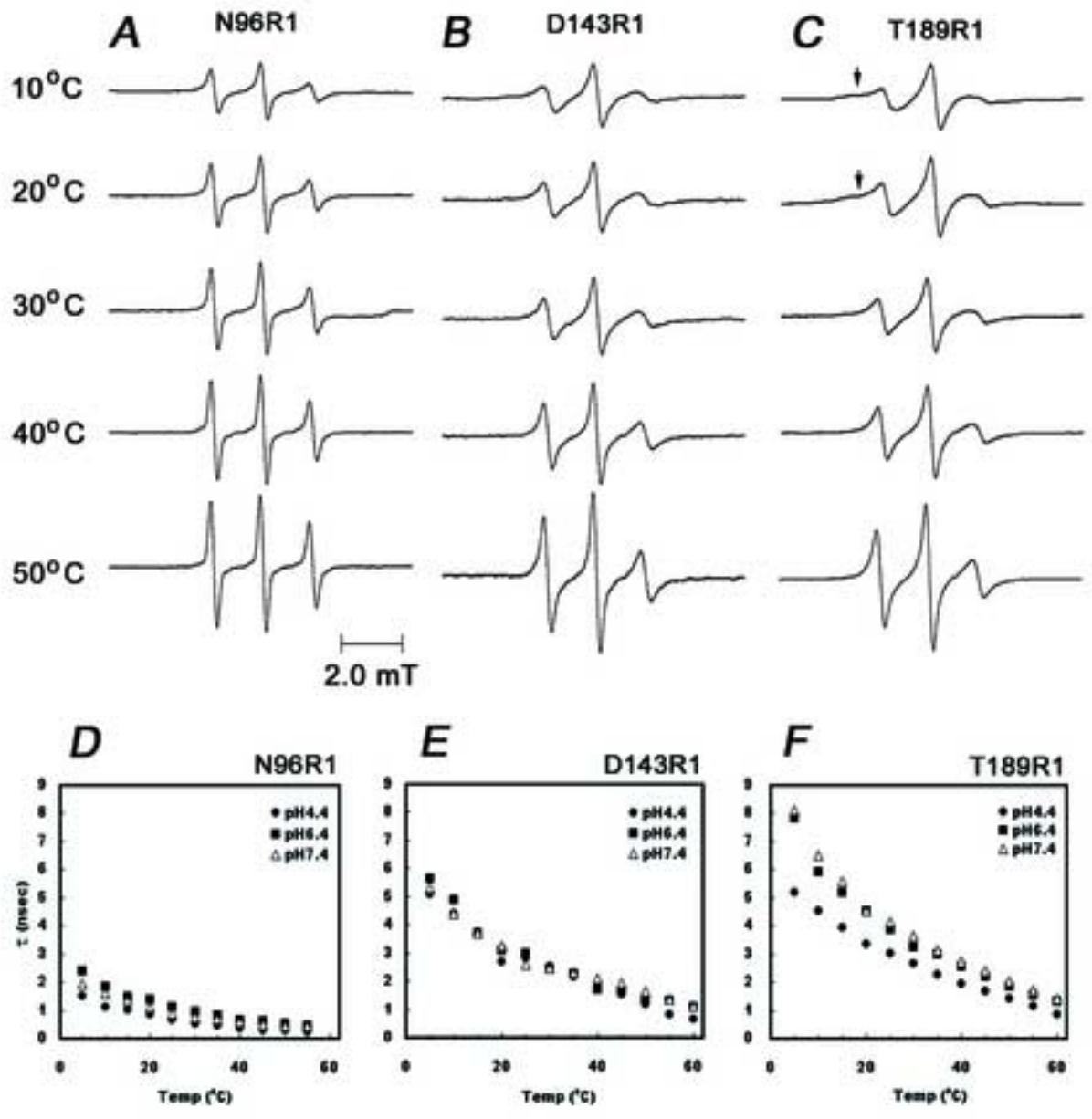

**Figure**

**Click here to download high resolution image**

Fig.5